NANO LETTERS

2005
Vol. 5, No. 10
1905−1909

Detecting Single Stranded DNA with a Solid State Nanopore

Daniel Fologea

Department of Physics, University of Arkansas, Fayetteville, Arkansas 72701

Marc Gershow

Department of Physics, Harvard University, Cambridge, Massachusetts 02138

Bradley Ledden

Department of Physics, University of Arkansas, Fayetteville, Arkansas 72701

David S. McNabb

Department of Biological Sciences, University of Arkansas, Fayetteville, Arkansas 72701

Jene A. Golovchenko

Department of Physics, Harvard University, Cambridge, Massachusetts 02138 and Division of Engineering and Applied Sciences, Harvard University, Cambridge, Massachusetts 02138

Jiali Li*

Department of Physics, University of Arkansas, Fayetteville, Arkansas 72701

Received June 24, 2005; Revised Manuscript Received August 15, 2005

ABSTRACT

Voltage biased solid-state nanopores are used to detect and characterize individual single stranded DNA molecules of fixed micrometer length by operating a nanopore detector at pH values greater than ~11.6. The distribution of observed molecular event durations and blockade currents shows that a significant fraction of the events obey a rule of constant event charge deficit (ecd) indicating that they correspond to molecules translocating through the nanopore in a distribution of folded and unfolded configurations. A surprisingly large component is unfolded. The result is an important milestone in developing solid-state nanopores for single molecule sequencing applications.

Single molecule methods based on nanopore detectors provide a new approach to rapid characterization and perhaps even sequencing of long biomolecules such as DNA.[1] Nanopores capable of single biomolecule detection fabricated from solid-state materials such as silicon nitride[2−5] or silicon dioxide[6,7] offer several potential advantages over biological pores, like alpha hemolysin, for which many elegant and beautiful single molecule results have already been reported.[1,8−16] These advantages include chemical, mechanical, and thermal robustness and the potential ability to articulate the solid-state nanopores with local electron tunneling and optical molecular probes. In order to one day apply these methods to rapid DNA sequencing, it is important to explore and understand the conditions under which long single stranded DNA (ss-DNA) molecules can be passed through and detected by solid-state nanopores.

Denaturation, or the transformation of double stranded DNA (ds-DNA) to ss-DNA, is routinely accomplished using alkaline pH and/or increased temperature.[17] These conditions are difficult if not impossible environments in which to operate biological nanopores. Here we show that a highly alkaline environment is compatible with the operation of a voltage biased silicon nitride nanopore, which enables the observation of freely translocating, long ss-DNA molecules through the nanopore. We find well defined ionic current blockades and translocation times for ss-DNA molecules that differ significantly from those of the same length ds-DNA molecules. The room-temperature denaturation of ds-DNA

* Corresponding author. E-mail: jialili@uark.edu.

10.1021/nl051199m CCC: $30.25
Published on Web 08/31/2005

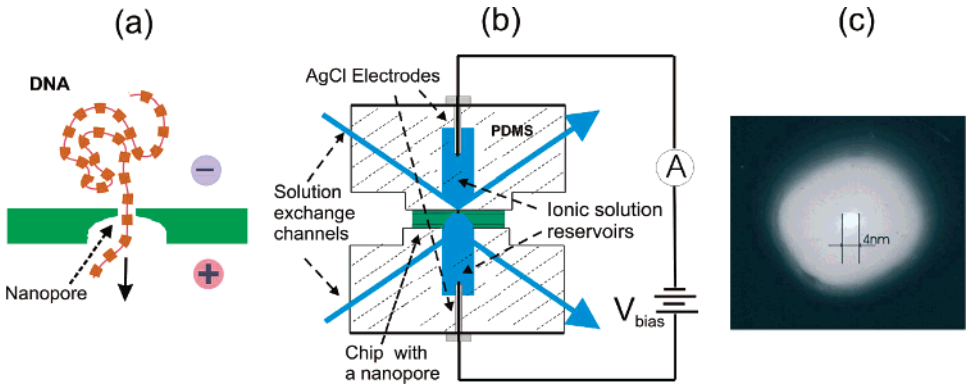

Figure 1. (a) Schematic illustration of DNA molecule translocating through a solid-state nanopore. (b) Experimental setup for single molecule measurements with a nanopore detector. (c) TEM of a silicon nitride nanopore, in this case 4 nm in diameter in a ~5−10 nm thick local membrane.

responsible for this difference is confirmed by optical absorption measurements.

A single molecule translocating through a nanopore is schematically illustrated in Figure 1a. The experimental setup is shown in Figure 1b. It consists of an ionic solution divided into two isolated reservoirs by an insulating silicon nitride membrane containing a single nanopore. An ionic current through the open nanopore is established by a voltage applied between silver/silver chloride electrodes placed in each of the two reservoirs. DNA molecules of interest are added to the reservoir with the negative electrode. They diffuse toward the nanopore and by virtue of their negative charge are captured by the local electric field near it.[18] The electric field within the nanopore then induces the molecule to pass through it to the positive reservoir. A time recording of the nanopore current during this event reveals the history of the molecule's interaction with the nanopore.

Nanopores used in this study were fabricated in free-standing 280 nm thick silicon nitride membranes supported by a 380 μm thick silicon chip using FIB milling followed by feedback controlled ion beam sculpting.[2,19] Figure 1c shows a TEM image of a 4 nm pore used in our studies. A voltage bias is applied and current measurements made with an Axopatch 200B patch clamp amplifier (Axon Instruments) operated with a 10 kHz low-pass Bessel filter. Additional features of our apparatus include an integrated flow system that allows for continuous and rapid interchange of solutions in the reservoirs and an open reservoir design that allows access to the solution for introduction of DNA and measurement of pH. For pH ~ 7, the nanopores can be operated stably in solution with ds-DNA for days, whereas at pH ~ 13, they are useable only for hours before increasing $1/f$ electronic noise, drifting baseline currents and permanent ss-DNA molecule blockages terminate the experiments.

The starting molecular material was ~3 kilobase-pair (kbp) ds-DNA, obtained from pSP65 plasmid (Promega Corp., Madison, WI). The plasmid was propagated in *E. coli* DH5α purified by Qiagen Plasmid Maxi kit (QIAGEN Inc., Valencia CA) and cleaved at a single site with the SmaI restriction enzyme to produce blunt-ended ds-DNA. The linearized plasmids were purified by two sequential phenol:chloroform (1:1 ratio) extractions, followed by one chloroform extraction, and finally precipitation with 2 volumes of ethanol. The purity and quantity of the recovered DNA was confirmed by agarose gel electrophoresis and UV absorbance. The prepared DNA was then re-suspended at a concentration of ~100 nM in TE buffer (10 mM Tris, 1 mM EDTA pH 7.5) (RT) and stored at −20 °C. The DNA was subsequently diluted to ~10 nM concentration in the negative chamber. The solution in both chambers was a 10 mM TE buffer (pH adjusted with KOH) with 1.6 M KCl, and 20 vol % glycerol. The glycerol increased the viscosity of the solution, slowing the DNA translocation through the nanopore.[20] This increased the length of single molecule events well beyond the rise time of the 10 kHz noise suppressing electronic filter.

Figure 2 shows nanopore DNA results for a bias voltage of 120 mV at pH 7 and 13 using the same 8 nm diameter solid-state nanopore. Panel (a) shows an event density plot of 3782 single molecule translocation signatures for the pH 7 ionic environment. The horizontal and vertical axes indicate the translocation time and mean ionic current blockage respectively, for each molecular event. The translocation time is the total time it takes an individual molecule to transit the pore. The ionic current blockage is the average decrease in nanopore ionic current during an event. The color represents the density of events at a given time and blockage. This two-dimensional histogram characterizes all events in the aggregate, but each event has a current vs time history that reveals information about the configuration of a single molecule as it passes through the nanopore. These are all recorded, and representative single molecule current−time traces for several events selected from the indicated region of the density plot are displayed as insets of Figure 2. No events are observed when no DNA is loaded in the solution.

The distribution of Figure 2a has a well-defined peak in translocation time at ~170 μs. The current blockage for these events is ~200 pA. When the pH is raised to 13, the results change dramatically, as indicated in Figure 2b (2905 events). An outline of the pH 7 data is included for comparison. The peak translocation time has dropped to ~120 μs and the peak current blockage to ~100 pA. Figure 2a corresponds to ds-

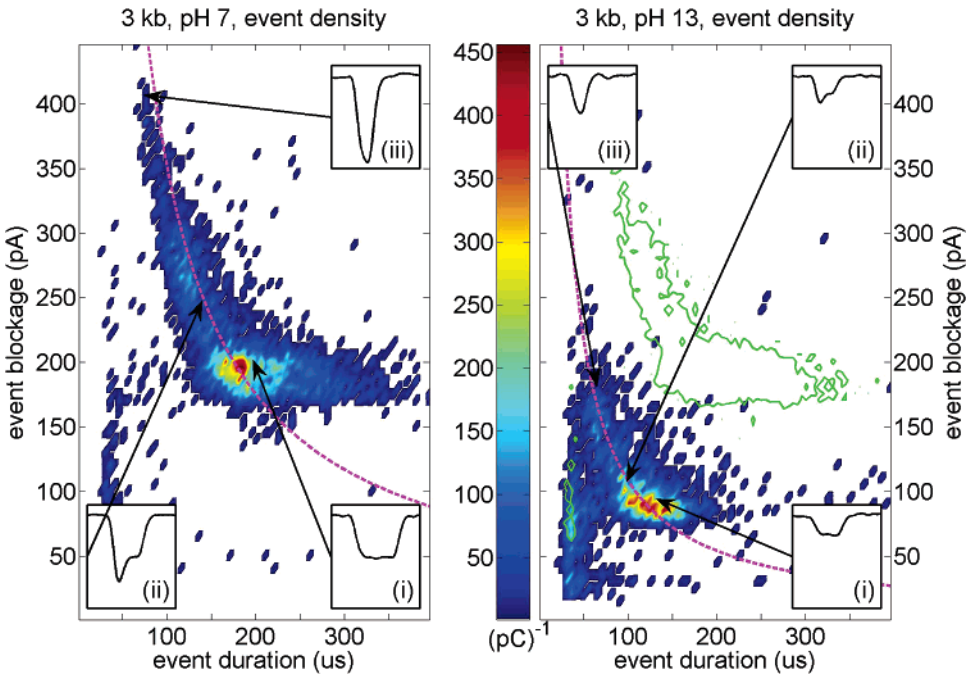

Figure 2. (a) Event density plot vs translocation time and average blockage current for 3 kb ss-DNA in pH 7 electrolyte solution. (b) pH 13 electrolyte solution. The dashed lines are hyperbolae of constant event charge deficit (see text). In panel b, the green outline of the data from panel a is presented to aid comparison. The color scale represents the probability density for a single event to occur at a given translocation time and blockage. Insets show representative time traces for individual events (i, unfolded molecule; ii, partially folded molecule; iii, completely doubled over molecule). The bounding box on each inset event is 400 us wide and 500 pA tall.

DNA and Figure 2b to ss-DNA in solution, a conclusion supported by optical experiments discussed below. Changing the pH for our salt solution produces only slight changes in ionic conductivity (<2%),

Inspection of Figure 2 shows that events whose translocation time falls below the most probable peak value generally have increased average current blockage values. This is consistent with the notion that some of the molecules pass through the pore folded (doubled over) on themselves.[3] The net electric force and the viscous drag are both doubled for a folded part of a molecule. This makes the velocity of a folded part of a molecule transiting the pore the same as that of an unfolded one. Thus in a time dt, twice the contour length passes for a folded region compared to an unfolded region. In addition, the instantaneous current blockage is proportional to the discrete number of strands of the folded molecule in the pore at any given time during an event. The distinct levels of current blockage during an event characterize the instantaneous state of the molecule's folding in the nanopore. (See insets of Figure 2 for examples of traces from unfolded, partly doubled over, and completely doubled over molecules for each pH.) The compensating effects of decreased translocation time and increased current blockage for folded molecules means that all molecules of the same length, regardless of folding, will produce current traces whose areas (time integral of the deviation from the baseline current) are equal.[3] We call this area the event charge deficit, ecd. Calling n the instantaneous number of strands in the pore, v the constant translocation velocity, ΔI_1 and τ_1 the current blockage and translocation time of an unfolded molecule respectively, and L the length of the molecule, the invariance of ecd to folding follows from

$$\begin{aligned}\text{ecd} &= \int_{\text{event}} \Delta I(t)\,\mathrm{d}t = \int_{\text{event}} n\Delta I_1\,\mathrm{d}t = \Delta I_1 \int_{\text{event}} n\,\mathrm{d}t \\ &= \Delta I_1 \int_{\text{event}} \frac{n}{\mathrm{d}L/\mathrm{d}t}\mathrm{d}L = \Delta I_1 \int_{\text{event}} \frac{n}{nv}\,\mathrm{d}L = \Delta I_1 \frac{L}{v} = \Delta I_1 \tau_1 \\ &= \text{const}\end{aligned}$$

Hyperbolae of constant ecd are shown as dashed lines in Figure 2. Events with translocation times at and below the most probable are seen to fall near this curve. This feature is a signature of the translocation of molecules folded in various configurations through the pore and cannot be explained by collisions of nontranslocating molecules with the pore, random noise, or filter effects. The detailed current−time traces provide information about where the folding occurs during the event. The peak in the distribution occurring on the long time low blockage part of the ecd curve corresponds to unfolded molecules.

The above argument applies only to molecules with viscosity limited motions through the pore that do not stick to its surface. We call these freely translocating. Those that do stick must have longer transit times and fail to follow curves of constant ecd in the event plots. Such events are seen in Figure 2; they have the same current blockage as the most probable ones, but longer durations. Thus we identify these events as molecules that temporarily stick to the walls of the nanopore during the translocation process. Earlier studies on ds-DNA show that this part of the

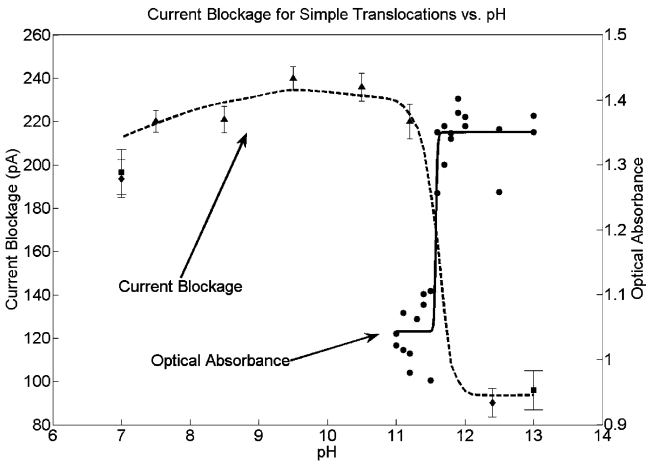

Figure 3. Plot of mean current blockage (for simple, unfolded, single level) events and DNA optical absorbance as a function of pH showing transition from ds to ss-DNA at pH ~11.5. The square markers represent the data from Figure 2, whereas the triangle and diamond markers represent experiments in two other pores including that in Figure 1c. The dashed line is a guide to the eye and not a fit.

distribution is greatly enhanced with very small nanopores.[3] The translocation times of these events are dominated by stochastic processes involving strong binding and unbinding between the DNA molecules and the walls of the pore. At this stage of nanopore science, the study of such events will yield more information about pore-molecule chemistry than about the properties of the biomolecules themselves.[21]

Analysis of event plots such as those in Figure 2 provides a great deal of evidence of, and information about, individual molecular translocations. The actual physical passage of DNA molecules between reservoirs through the nanopore is also established by observations of events for molecules returning to the starting reservoir upon bias voltage reversal. These signals are observed only after hours of operation in the forward bias condition.

Figure 3 presents a plot of the most probable current blockage for unfolded translocations obtained in a series of experiments where the pH was changed in steps between 7 and 13. These measurements were made with the expectation that a drop in this current blockage would occur abruptly at the room-temperature pH where the DNA denatures, because a single stranded molecule should be less effective in blocking the area of the nanopore. Although it is well-known that the stability of the ds-DNA helix is reduced at high pH, and at high enough pH the single stranded state is favored,[22] we were not able to find the value for the room temperature denaturing pH in the literature for the high salt concentrations of our experiments (see ref 22 for melting curves in 250 mM NaCl at pHs up to 10.6). Thus, we also measured the room temperature DNA optical absorbance at 260 nm as a function of pH in 1.6 M KCl with 20% glycerol. As seen in Figure 3, the absorbance increases abruptly by ~30% at pH 11.6. This is caused by the well documented hyperchromicity of DNA[22,23] upon denaturation. Thus, the relatively constant blockade current up to pH 11.2 and its subsequent drop at pH 12.2 and 13, where no properties of the nanopore change dramatically, is associated with denaturation. This confirms that ss-DNA is responsible for the results shown in Figure 2b.

Discussion

The events we observe have a well-defined duration and average current blockage and are similar to those that previous studies have identified with translocating molecules.[3,7] The current trace for each event shows quantized blockages with shorter events composed of regions with deeper current blockage. Event distributions such as those in Figure 2 have a well-defined peak and a hyperbolic tail of events with constant ecd extending to lower translocation times and larger average blockages. We are unable to conceive of any explanation for these features other than the peak of the distribution corresponding to extended DNA molecules passing single file through the nanopore and the tail to molecules having various folded configurations where multiple strands of the same molecule can simultaneously occupy the pore at some time during the translocation. These features are observed at both low and high pH, confirming the translocation of double stranded and pH melted single stranded DNA through the same nanopore. The ubiquity of unfolded molecular events (> 50%) even for nanopores of ~10 nm in diameter suggests that long molecules are often unfolded by the nanopore capture process itself and that extremely small "molecule hugging" pores are not necessary to linearize DNA molecules as they translocate through the nanopore.[3,5]

We have referred above to events that fall on hyperbolas of constant ecd as "free translocations". For freely translocating molecules the translocation time and ecd is determined primarily by the identity, length and charge state of the molecule, the applied electric field, and viscous drag in the fluid within and around the pore. The results presented here regarding translocation times and current blockages for freely translocating ds-DNA are consistent with previous experiments[3,7] when the effect of the glycerol is taken into account. The translocation time ratio for 0% glycerol ds-DNA[3] to 20% glycerol ds-DNA is 105 μs/170 μs which is remarkably close to the ratio of viscosities, 1.0 cp/1.68 cp. For ss-DNA in alkaline conditions, both current drop and translocation time are reduced. Both parameters are related to the ratio of the ss to ds-DNA molecule areas which is nominally ~2/1. In this way, we can account for reduced current drop for ss-DNA under the same ionic salt conditions. For translocation time, other factors, including effective charge density, viscous drag forces, and persistence length differences, should be considered in a further analysis of ss-DNA translocation times.

In conclusion, our experiment demonstrates conclusively that long denatured single stranded DNA molecules can be observed to freely translocate in stretched out configurations through a solid-state nanopore. This bodes well for the merging of nanopore based molecule manipulation with molecular electronics methods for single base resolution sequencing via the incorporation of local nanoscale electrodes

in the nanopore. Our results also demonstrate the new and unique ability of a nanopore to detect single molecule hybridization without the use of fluorescent labels.

Acknowledgment. We acknowledge Dr. Qun Cai, Dr. Toshiyuki Mitsui's assistance with nanopore preparation, and valuable discussions with Prof. Daniel Branton. Support for this research has been provided by NIH, DOE, ABI, and the University of Arkansas start-up fund.

References

(1) Kasianowicz, J. J.; Brandin, E.; Branton, D.; Deamer, D. W. *Proc. Natl. Acad. Sci. U.S.A.* **1996**, *93*, 13770−13773.
(2) Li, J.; Stein, D.; McMullan, C.; Branton, D.; Aziz, M. J.; Golovchenko, J. A. *Nature* **2001**, *412*, 166−169.
(3) Li, J.; Gershow, M.; Stein, D.; Brandin, E.; Golovchenko, J. A. *Nat. Mater.* **2003**, *2*, 611−615.
(4) Stein, D.; Li, J.; Golovchenko, J. A. *Phys. Rev. Lett.* **2002**, *89*, 276106(4).
(5) Chen, P.; Jiajun, G.; Brandin, E.; Young-Rok, K.; Wang, Q.; Branton, D. *Nano Lett.* **2004**, *4*, 2293−2298.
(6) Storm, A. J.; Chen, J. H.; Ling, X. S.; Zandbergen, H. W.; Dekker, C. *Nat. Mater.* **2003**, *2*, 537−540.
(7) Storm, A. J.; Storm, C.; Chen, J.; Zandbergen, H.; Joanny, J.-F.; Dekker, C. *Nano Lett.* **2005**, *5*, 1193−1197.
(8) Bezrukov, S. M.; Vodyanoy, I.; Parsegian, V. A. *Nature* **1994**, *370*, 279−281.
(9) Akeson, M.; Branton, D.; Kasianowicz, J. J.; Brandin, E.; Deamer, D. W. *Biophys. J.* **1999**, *77*, 3227−3233.
(10) Henrickson, S. E.; Misakian, M.; Robertson, B.; Kasianowicz, J. J. *Phys. Rev. Lett.* **2000**, *85*, 3057−3060.
(11) Meller, A.; Nivon, L.; Brandin, E.; Golovchenko, J.; Branton, D. *Proc. Natl. Acad. Sci. U.S.A.* **2000**, *97*, 1079−1084.
(12) Kasianowicz, J. J.; Henrickson, S. E.; Weetall, H. H.; Robertson, B. *Anal. Chem.* **2001**, *73*, 2268−2272.
(13) Vercoutere, W.; Winters-Hilt, S.; Olsen, H.; Deamer, D.; Haussler, D.; Akeson, M. *Nat. Biotechnol.* **2001**, *19*, 248−252.
(14) Meller, A.; Nivon, L.; Branton, D. *Phys. Rev. Lett.* **2001**, *86*, 3435−3438.
(15) Meller, A. *J. Phys.: Condens. Matter* **2003**, *15*, R581−R607.
(16) Nakane, J. J.; Akeson, M.; Marziali, A. *J. Phys.: Condens. Matter* **2003**, *15*, R1365−R1393.
(17) Lehninger, A. L.; Nelson, D. L.; Cox, M. M. *Principles of Biochemistry*; Worth Publishers Inc.: New York, 1993; pp 330−342.
(18) Ambjornsson, T.; Apell, S. P.; Konkoli, Z.; Di Marzio, E. A.; Kasianowicz, J. J. *J. Chem. Phys.* **2002**, *117*, 4063−4073.
(19) Stein, D.; McMullan, C. J.; Li, J.; Golovchenko, J. A. *Rev. Sci. Instrum.* **2004**, *75*, 900−905.
(20) Fologea, D.; Uplinger, J.; Thomas, B.; McNabb, D. S.; Li, J. *Nano Lett.*, In Press.
(21) Heng, J. B.; Ho, C.; Kim, T.; Timp, R.; Aksimentiev, A.; Grinkova, Y. V.; Sligar, S.; Schulten, K.; Timp, G. *Biophys. J.* **2004**, *87*, 2905−2911.
(22) Bloomfield, V. A.; Crothers, D. M.; Tinoco, I., Jr. *Physical Chemistry of Nucleic Acids*; Harper & Row: New York, 1974; pp 294−371.
(23) Williams, M. C.; Wenner, J. R.; Rouzina, I.; Bloomfield, V. A. *Biophys. J* **2001**, *80*, 874−881.

NL051199M